

Theory of the angle-resonant polariton amplifier

C. Ciuti,¹ P. Schwendimann,² B. Deveaud,¹ and A. Quattropani¹

¹Physics Department, Swiss Federal Institute of Technology Lausanne, CH-1015 Lausanne-EPFL, Switzerland

²Defense Procurement, System Analysis Division, CH-3003 Bern, Switzerland

(Received 12 June 2000)

A microscopic theory is presented for the giant amplification from microcavities in the strong exciton-photon coupling regime, providing excellent agreement with recent angle-resolved pump-probe experiments. The analytical and numerical solutions give insight into the physics of the polariton parametric amplifier. The coherent gain, due to polariton four-wave-mixing, has a threshold dependence on the pump power and is spectrally blueshifted from the lower polariton energy. The gain shift does not depend on the power, but on the unperturbed polariton linewidth.

Since the observation of the strong-coupling regime between quantum-well excitons and microcavity photons,¹ semiconductor microcavities have been the subject of a very active research.² The mixed exciton-photon modes, called polaritons, have a quasi-two-dimensional character due to the translational invariance in the microcavity embedded quantum-well plane, while the motion is confined (quantized) in the orthogonal direction. The polariton modes with in-plane wave vector \mathbf{k} can be excited by external photons which are sent to the planar structure with a finite incidence angle θ , such as to have the same in-plane wave-vector component.³ In principle, polaritons are fascinating quasiparticles, because they share at the same time the very sharp energy dispersion of the cavity photons and the pronounced electronic nonlinearities of excitons.

Many of the experiments in semiconductor microcavities have studied the role of the collision broadening and the bleaching of the exciton resonance in the transition from the strong to the weak exciton-photon coupling regime.^{4,5} More recently, several publications have reported nonlinear emission from microcavities in the strong-coupling regime.⁶⁻⁹ In particular, Savvidis *et al.*⁸ have uncovered huge light amplification (≈ 100) through angle-resolved pump-probe experiments. When a pump pulse with incidence angle θ_p (in-plane wave vector \mathbf{k}_p) excites resonantly the lower polariton branch and a probe beam is taken at normal incidence (in-plane wave vector $\mathbf{k}=\mathbf{0}$), the probe amplification occurs at the critical angle such that $2E_{LP}(k_p)=E_{LP}(0)+E_{LP}(2k_p)$, where E_{LP} is the lower polariton energy. This experimentally demonstrates the existence of a very efficient all-optical amplifier through polaritons.

Apart from the natural need of a theory for such a remarkable effect, many and relevant questions have still to be answered. Which is the role of the phase-coherent polarization in the stimulated amplification process? Why does the gain spectrally occur blueshifted with respect to the unperturbed lower polariton? Why is the shift power independent? What determines the maximum gain?

In this paper, we present a theory for the polariton parametric amplifier that explains the very recent observation of giant polariton amplification and answers all the crucial questions above mentioned. The interacting polariton system is treated starting from a microscopic Hamiltonian including

exciton-exciton interaction and exciton saturation.¹⁰⁻¹⁵ The analytical and numerical solutions lead to unexpected, but simple quantitative relations for the threshold condition, spectral properties, and overall efficiency of the amplification, opening the way to further significant developments.

In the following, we focus on angle-resolved pump-probe spectroscopy with co-circularly polarized beams (e.g., $\sigma_+\sigma_+$). The free Hamiltonian for excitons and cavity photons is

$$H_0 = \sum_{\mathbf{k}} E_X(k) b_{+,\mathbf{k}}^\dagger b_{+,\mathbf{k}} + \sum_{\mathbf{k}} E_C(k) a_{+,\mathbf{k}}^\dagger a_{+,\mathbf{k}}.$$

The operator $b_{+,\mathbf{k}}^\dagger$ creates an exciton with spin σ_+ and in-plane wave-vector \mathbf{k} , while $a_{+,\mathbf{k}}^\dagger$ is the analogous one for the cavity photon. The quantities $E_X(k)$ and $E_C(k)$ are the energy dispersions for exciton and cavity mode respectively. The linear coupling between exciton and cavity photon is represented by the term $H_{XC} = \sum_{\mathbf{k}} \hbar \Omega_R a_{+,\mathbf{k}}^\dagger b_{+,\mathbf{k}} + \text{H.c.}$, where $2\hbar \Omega_R$ is the vacuum Rabi splitting. The operator $b_{+,\mathbf{k}}$ satisfies boson commutation rules, but the fermionic nature of electrons and holes is accounted for through the exciton-exciton interaction and exciton saturation. The Coulomb interaction between carriers is responsible for an effective exciton-exciton interaction that reads

$$H_{XX} = \frac{1}{2} \sum_{\mathbf{k}, \mathbf{k}', \mathbf{q}} V_q^{\text{eff}} b_{+,\mathbf{k}+\mathbf{q}}^\dagger b_{+,\mathbf{k}'}^\dagger b_{+,\mathbf{k}-\mathbf{q}} b_{+,\mathbf{k}+\mathbf{k}'}.$$

The exciton and cavity photon are strongly coupled for wave vectors much smaller than $1/\lambda_X$, where λ_X is the two-dimensional exciton radius. We point out that for $q\lambda_X \ll 1$, $V_q^{\text{eff}} \approx V_0^{\text{eff}} = 6e^2\lambda_X/(\epsilon_0 A)$ with ϵ_0 the dielectric constant of the quantum well and A the macroscopic quantization area. The composite nature of the exciton quasiparticles manifests itself in an anharmonic saturation term in the light-exciton coupling

$$H_{XC}^{\text{sat}} = - \sum_{\mathbf{k}, \mathbf{k}', \mathbf{q}} \frac{\hbar \Omega_R}{n_{\text{sat}} A} a_{+,\mathbf{k}+\mathbf{q}}^\dagger b_{+,\mathbf{k}'}^\dagger b_{+,\mathbf{k}-\mathbf{q}} b_{+,\mathbf{k}+\mathbf{k}'} + \text{H.c.},$$

where $n_{\text{sat}} = 7/(16\pi\lambda_X^2)$ is the exciton saturation density. Finally, the coupling to the external radiation field is

accounted for within the quasimode Hamiltonian $H_{field} = \{g \sum_{\mathbf{k}} \hbar \Omega_{+, \mathbf{k}}(t) a_{+, \mathbf{k}}^\dagger + \text{H.c.}\}$. The quantity g is the quasimode coupling constant, while $\hbar \Omega_{+, \mathbf{k}}(t)$ is the Rabi energy of the external electromagnetic field.

The experiments we want to model are such that the pump is spectrally narrow and resonantly excites the lower polariton branch. Therefore, in such a situation it is possible to neglect nonlinear contributions related to the upper polariton branch and consider only the lower polariton states. The lower polariton annihilation operator is $p_{\mathbf{k}} = X_{\mathbf{k}} b_{+, \mathbf{k}} + C_{\mathbf{k}} a_{+, \mathbf{k}}$, where $X_{\mathbf{k}}$ and $C_{\mathbf{k}}$ are the Hopfield coefficients for the exciton and cavity fraction, respectively. The coefficients are real and such that $X_{\mathbf{k}} > 0$ and $C_{\mathbf{k}} < 0$. In terms of the lower polariton operators, our model Hamiltonian is $H = H_{LP} + H_{PP}^{eff} + H_{qm}$. The free polariton term is $H_{LP} = \sum_{\mathbf{k}} E_{LP}(k) p_{\mathbf{k}}^\dagger p_{\mathbf{k}}$ with $E_{LP}(k)$ the lower polariton energy dispersion. The effective polariton-polariton interaction term reads

$$H_{PP}^{eff} = \frac{1}{2} \sum_{\mathbf{k}, \mathbf{k}', \mathbf{q}} \frac{\lambda_X^2}{A} V_{\mathbf{k}, \mathbf{k}', \mathbf{q}}^{PP} p_{\mathbf{k}+\mathbf{q}}^\dagger p_{\mathbf{k}'-\mathbf{q}}^\dagger p_{\mathbf{k}} p_{\mathbf{k}'}.$$

The effective potential for the polariton-polariton interaction, coming from the exciton-exciton interaction and exciton saturation, is

$$V_{\mathbf{k}, \mathbf{k}', \mathbf{q}}^{PP} = \left\{ \frac{6e^2}{\epsilon \lambda_X} X_{\mathbf{k}+\mathbf{q}} X_{\mathbf{k}'} + 2 \frac{\hbar \Omega_R}{n_{sat} \lambda_X^2} \times (|C_{\mathbf{k}+\mathbf{q}}| X_{\mathbf{k}'} + |C_{\mathbf{k}'}| X_{\mathbf{k}+\mathbf{q}}) \right\} X_{\mathbf{k}'-\mathbf{q}} X_{\mathbf{k}}.$$

Finally, we have the quasimode Hamiltonian in the polariton basis $H_{qm} = \{g \sum_{\mathbf{k}} \hbar \Omega_{+, \mathbf{k}}(t) C_{\mathbf{k}} p_{\mathbf{k}}^\dagger + \text{H.c.}\}$.

Let us now consider an excitation configuration with the probe at normal incidence and the pump at a finite incidence angle. Namely, we have $\Omega_{+, \mathbf{k}}(t) = \delta_{\mathbf{k}, \mathbf{k}_p} \Omega_{pump}(t) + \delta_{\mathbf{k}, \mathbf{0}} \Omega_{probe}(t)$. The optical response of the probe beam is given by the expectation value $\langle p_{\mathbf{0}} \rangle$, that is the polarization of the σ_+ lower polariton with in-plane wave vector $\mathbf{k} = \mathbf{0}$. Such a quantity is coupled through polariton-polariton interaction to $\langle p_{\mathbf{k}_p} \rangle$, that is the polarization induced by the pump. The polariton-polariton diffusion produces a wave-mixing component at the idler wave vector $2\mathbf{k}_p$. When one neglects all terms of order higher than one in the probe field and factorizes all the many-operator expectation values in products of $\langle p_{\mathbf{0}} \rangle$, $\langle p_{\mathbf{k}_p} \rangle$, $\langle p_{2\mathbf{k}_p} \rangle$, it is possible to obtain a close set of equations for the three expectation values mentioned above. It is convenient to consider the rescaled quantity $P_{\mathbf{k}} = \langle p_{\mathbf{k}} \rangle \lambda_X / \sqrt{A}$. Note that $|P_{\mathbf{k}}|^2 = n_{\mathbf{k}} \lambda_X^2$, where $n_{\mathbf{k}}$ is the coherent density (per unit area) of lower polaritons with wave vector \mathbf{k} . Thus, the equation of motion for the polarization at the probe wave vector is

$$\frac{\partial P_{\mathbf{0}}}{\partial t} = \frac{i}{\hbar} \{ [\tilde{E}_{LP}(0) + i\gamma] P_{\mathbf{0}} + E_{int} P_{\mathbf{0}}^* P_{2\mathbf{k}_p}^2 + \mathcal{F}_{probe}(t) \}. \quad (1)$$

The driving term is $\mathcal{F}_{probe}(t) = (\lambda_X / \sqrt{A}) g C_{\mathbf{0}} \hbar \Omega_{probe}(t)$, while the coupling energy is $E_{int} = \frac{1}{2} (V_{\mathbf{k}_p, \mathbf{k}_p, \mathbf{k}_p}^{PP} + V_{\mathbf{k}_p, \mathbf{k}_p, -\mathbf{k}_p}^{PP})$.

The polarization at the probe wave vector is resonant at the blueshifted energy $\tilde{E}_{LP}(0) = E_{LP}(0) + 2V_{\mathbf{0}, \mathbf{k}_p, \mathbf{0}}^{PP} |P_{\mathbf{k}_p}|^2$. The blueshift is due to the polariton-polariton interaction. The energy 2γ is the polariton linewidth [full width at half maximum (FWHM)]. The equation for the pump reads

$$\frac{\partial P_{\mathbf{k}_p}}{\partial t} = \frac{i}{\hbar} \{ (\tilde{E}_{LP}(k_p) + i\gamma) P_{\mathbf{k}_p} + 2E_{int} P_{\mathbf{k}_p}^* P_{\mathbf{0}} P_{2\mathbf{k}_p} + \mathcal{F}_{pump}(t) \}. \quad (2)$$

The pump field is $\mathcal{F}_{pump}(t) = (\lambda_X / \sqrt{A}) g C_{\mathbf{k}_p} \hbar \Omega_{pump}(t)$. The polarization at the pump wave vector is resonant at the renormalized energy $\tilde{E}_{LP}(k_p) = E_{LP}(k_p) + 2V_{\mathbf{k}_p, \mathbf{k}_p, \mathbf{0}}^{PP} |P_{\mathbf{k}_p}|^2$. Finally, the equation for the idler polarization reads

$$\frac{\partial P_{2\mathbf{k}_p}}{\partial t} = \frac{i}{\hbar} \{ [\tilde{E}_{LP}(2k_p) + i\gamma] P_{2\mathbf{k}_p} + E_{int} P_{\mathbf{0}}^* P_{\mathbf{k}_p}^2 \}, \quad (3)$$

with $\tilde{E}_{LP}(2k_p) = E_{LP}(2k_p) + 2V_{2\mathbf{k}_p, \mathbf{k}_p, \mathbf{0}}^{PP} |P_{\mathbf{k}_p}|^2$. Of course, there is no external driving field for the idler.

Concerning the solution of the polariton amplifier equations, we proceed in two steps. First, we extract the salient physical features by finding analytical results for the steady-state regime. Second, we provide numerical results for the pulsed excitation case. Let us start with the analytical treatment of the steady-state case. In the rotating frame approximation, the pump polarization is $P_{\mathbf{k}_p}(t) = \bar{P}_{\mathbf{k}_p} e^{i\omega_p t}$ and the cw-probe field reads $\mathcal{F}_{probe}(t) = \bar{\mathcal{F}}_{probe} e^{i\omega t}$. Consequently, the stationary solutions for the probe and idler polarizations have the form $P_{\mathbf{0}} = \bar{P}_{\mathbf{0}} e^{i\omega t}$ and $P_{2\mathbf{k}_p} = \bar{P}_{2\mathbf{k}_p} e^{i(2\omega_p - \omega)t}$. Taking Eq. (1) and the complex conjugated of Eq. (3), we have the linear inhomogeneous system that determines the quantities $\bar{P}_{\mathbf{0}}$ and $\bar{P}_{2\mathbf{k}_p}^*$ as a function of $\bar{P}_{\mathbf{k}_p}$. We point out that such equations are analogous to that involved in the parametric amplifier model.¹⁶ With simple algebra, we find that the probe polarization spectrum has two poles, namely $\bar{P}_{\mathbf{0}} \propto 1/[(E_- - \hbar\omega) \times (E_+ - \hbar\omega)]$, where the complex energies of the poles are

$$E_{\pm} = \frac{\tilde{E}_{LP}(0) + 2\hbar\omega_p - \tilde{E}_{LP}(2k_p)}{2} + i\gamma \pm \frac{1}{2} \sqrt{\Theta},$$

with $\Theta = (\tilde{E}_{LP}(0) + \tilde{E}_{LP}(2k_p) - 2\hbar\omega_p)^2 - 4(E_{int} |\bar{P}_{\mathbf{k}_p}|^2)^2$. The nonlinear response of the probe becomes singular when one of the two poles is real. Such a condition is fulfilled when $\tilde{E}_{LP}(0) + \tilde{E}_{LP}(2k_p) - 2\hbar\omega_p = 0$ (energy conservation for the wave mixing) and for a *threshold density* such as $E_{int} |\bar{P}_{\mathbf{k}_p}|^2 = \gamma$. This way, E_- becomes real and $E_- - E_{LP}(0) = 2\gamma V_{\mathbf{0}, \mathbf{k}_p, \mathbf{0}}^{PP} / E_{int} \approx 2\gamma$, while $E_+ = E_- + i2\gamma$. This implies that *the gain peak energy is blueshifted with respect to the unperturbed lower polariton and does not depend on the pump intensity*. When the energy conservation is not satisfied, the threshold density is higher and the amplification clearly smaller. As in the parametric amplifier model,¹⁶ the singularity of the probe polarization at $\hbar\omega = \tilde{E}_{LP}(0)$ is only formal and becomes finite when the equation for the pump is consistently solved. In fact, the pump polarization $\bar{P}_{\mathbf{k}_p}$ is not independent from $\bar{P}_{\mathbf{0}}$.

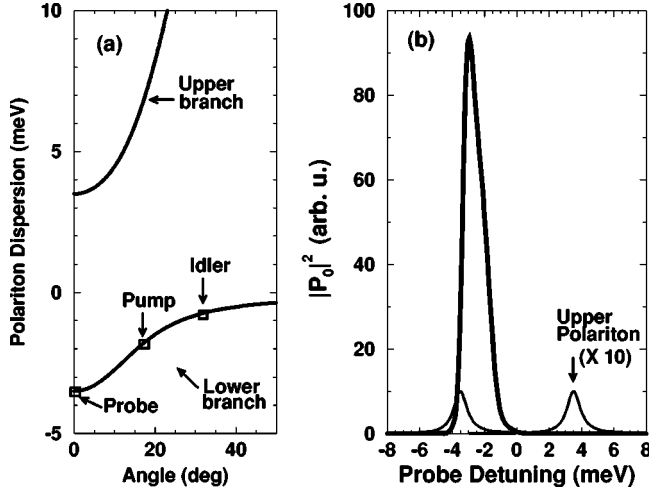


FIG. 1. (a) Polariton energy dispersion (meV) versus angle (deg). (b) $|P_0(\omega)|^2$ (arb. units) versus probe detuning $\hbar\omega - E_X$ (meV) for pump intensities (arb. units I_0). Pump angle: $\theta_p = 16^\circ$. Probe intensity: $I_{probe} = 10^{-3}I_0$. Thin solid line: signal (enlarged 10 times) without pump. The upper polariton peak is shown as a reference. Thick line: $I_{pump} = I_0$. Other parameters in the text.

The enlightening results for the steady-state regime allow to understand the basic physics also for the pulsed excitation. To complete the study, we solve numerically Eqs. (1), (2), and (3) for a realistic GaAs microcavity system with Rabi splitting $2\hbar\Omega_R = 7$ meV and polariton broadening $\gamma = 0.5$ meV. We take a resonant pump pulse (3 ps is the intensity FWHM) and probe the system with a broad-band 100-fs pulse. We choose the pump wave vector such as to satisfy the energy conservation condition $E_{LP}(0) + E_{LP}(2k_p) = 2E_{LP}(k_p)$ and tune the pump spectrally resonant with the lower polariton branch at the same angle [$\hbar\omega_p = E_{LP}(k_p)$]. The pump incidence angle θ_p is defined by the relation $k_p = \omega_p/c \sin \theta_p$. In the considered case, the angle satisfying the energy conservation is nearly 15° [see Fig. 1(a)]. In Fig. 1(b), we show the results for the frequency-dependent quantity $|P_0(\omega)|^2$, that is the spectrum of the squared polarization at the probe wave vector. The thin line represents the case without pump. When a threshold intensity is reached, enormous amplification occurs. The spectral line shape is strongly asymmetric. The peak energy of the spectrum does not coincide with the mean energy $E_{mean} = \{\int d\omega \hbar\omega |P_0(\omega)|^2\} / \{\int d\omega |P_0(\omega)|^2\}$. In the regime of strong gain, E_{mean} does not depend on the pump intensity, but only on the polariton linewidth. In fact, we have carefully verified that E_{mean} coincides with the pole energy E_- of the steady-state case.

In Fig. 2 we show the spectrally integrated gain as a function of the pump incidence angle [$\hbar\omega_p = E_{LP}(k_p)$ for each angle]. The gain is actually resonant around the angle satisfying the energy conservation condition. As a function of intensity the peak angle slightly shifts due to the renormalization of the polariton energies.

In Fig. 3(a), the net gain is shown as a function of the pump intensity. The gain presents an abrupt threshold. For higher intensities, it increases up to a maximum of the order of 10^2 and then saturates. In the range of gain between 10^{-1} and 10^2 , the intensity dependence of the gain is hardly distinguishable from an exponential. *The efficiency of the am-*

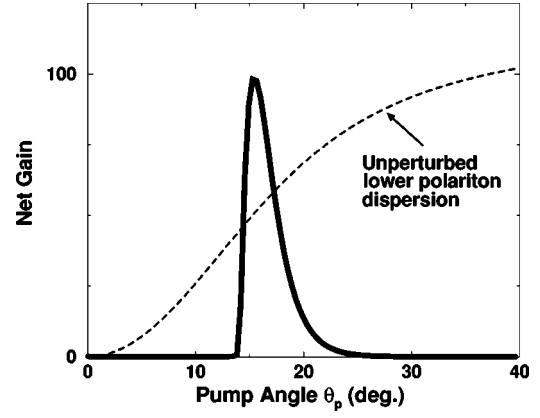


FIG. 2. Spectrally integrated gain versus pump incidence angle (deg). Same parameters as in Fig. 1. The dashed-line represents the shape of the unperturbed lower polariton angular dispersion.

plifier is dramatically sensitive to the polariton broadening. The dashed line shows that when the broadening is increased by a factor of 2, the threshold intensity is increased by a factor of 2 and the maximum gain is decreased by nearly an order of magnitude. In Fig. 3(b), the dependence on the probe intensity I_{probe} is shown. For I_{probe} tending to I_{pump} , the amplification decreases, because the gain is intrinsically limited by the finite density of polaritons created by the pump.

The coherent nature of the amplification is clearly shown in Fig. 4(a) where the net gain (solid line) is plotted versus the pump-probe delay. In panel (b), the quantity $|P_{k_p}|^2 / (n_{sat} \lambda_X^2)$ is shown as a function of time. This quantity represents the coherent density of polaritons at the pump wave-vector in units of the exciton saturation density n_{sat} . The dashed line represents the results without probe, while the solid line is obtained with $I_{probe} = 0.1I_{pump}$. In this case, the relatively intense probe induces a macroscopic transfer ($\approx 10\%$) of polaritons from the pump wave vector \mathbf{k}_p to $\mathbf{0}$ and $2\mathbf{k}_p$. It is worth pointing out that our results are not only in excellent agreement with the whole rich phenomenology of the experiments by Savvidis *et al.*,⁸ but give a precise description of the conditions to achieve the gain threshold,

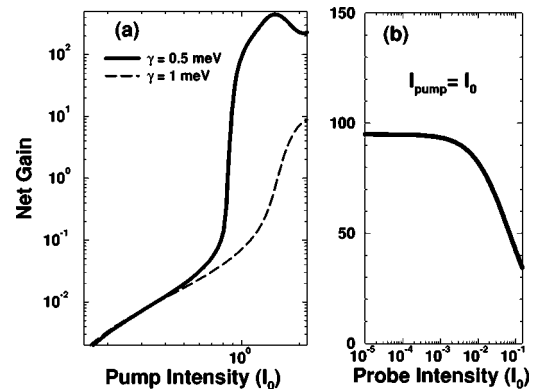


FIG. 3. (a) Spectrally integrated gain (log scale) versus pump intensity I_{pump} (log scale, I_0 units) at $\theta_p = 16^\circ$ for two different polariton linewidths. Solid line: $\gamma = 0.5$ meV. Dashed line: $\gamma = 1$ meV. (b) Net gain versus probe intensity I_{probe} (log scale, I_0 units).

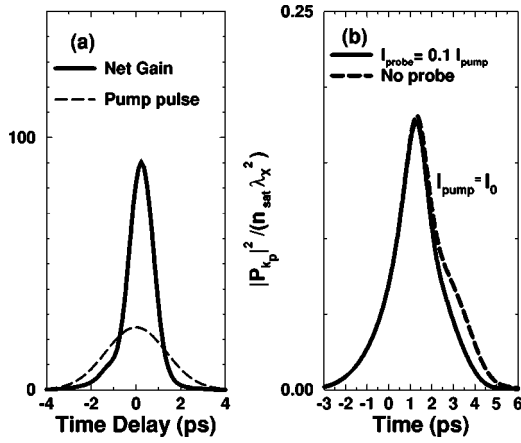


FIG. 4. (a) Solid line: net gain versus pump-probe delay (ps) for $I_{pump} = I_0$ and $I_{probe} = 10^{-3} I_{pump}$. Dashed line: pump intensity (arb. units) as a function of time. (b) $|P_{kp}|^2 / (n_{sat} \lambda_x^2)$ as a function of time (ps). Solid line: $I_{probe} = 0.1 I_0$. Dashed line: no probe.

explain the nontrivial spectral features, and the dominant role of the polariton linewidth in determining the maximum value of the gain.

Finally, we add some additional remarks about the nonlinearities in experiments without probe beam. It is known that the spontaneous emission can act as a spontaneous probe. The wave mixing of a spontaneous probe with an applied pump beam is known as hyper-Raman scattering.¹⁷ Houdré *et al.*⁹ have recently observed giant nonlinear emission of lower polaritons in cw experiments where the pump resonantly excites the lower polariton branch at the angle

satisfying the energy conservation condition for the wave mixing. Moreover, the spectral shift of the nonlinear emission is just the the polariton linewidth in perfect agreement with our analytical result for the cw case. Unlike Refs. 8 and 9, the experiments in Refs. 6 and 7 have been performed with a nonresonant pump. In such a case, the incoherent dynamics and the contribution of the upper polariton branch have to be considered, complicating enormously the theoretical description. Since the phenomenology and spectral features are reminiscent of the resonant and coherent case, further investigation is encouraged in this direction.

In conclusion, we have presented microscopic equations for the polariton parametric amplifier, whose solutions are in excellent agreement with recent experiments.^{8,9} The polariton linewidth plays a key role in determining the threshold for the amplification, the spectral shift, and the maximum value of the gain. Our theory gives a new perspective to the current debate on the microcavity nonlinear optics, showing in a clear way the intrinsic polariton nonlinearities and provides a powerful, manageable theoretical tool for further investigations.

We acknowledge discussions with G. Bongiovanni, I. Carusotto, M.A. Dupertuis, R. Girlanda, G. Hayes, C. Piermarocchi, F. Quochi, G. Rochat, M. Saba, P. Savvidis, R.P. Stanley, J.L. Staehli, V. Savona, and C. Weisbuch. We thank J. Baumberg and R. Houdré for transmission of experimental results prior to publication. Special thanks to S. Savasta and F. Tassone for enthusiastic and critical reading of the manuscript.

¹C. Weisbuch *et al.*, Phys. Rev. Lett. **69**, 3314 (1992).

²For a review see V. Savona *et al.*, *New Aspects in Optical Properties of Nanostructures, Phase Transitions* (Gordon and Breach, New York, 1998); G. Khitrova *et al.*, Rev. Mod. Phys. **71**, 1591 (1999).

³R. Houdré *et al.*, Phys. Rev. Lett. **73**, 2043 (1994).

⁴M. Kira *et al.*, Phys. Rev. Lett. **79**, 5170 (1997).

⁵F. Quochi *et al.*, Phys. Rev. Lett. **80**, 4733 (1998).

⁶P. Senellart and J. Bloch, Phys. Rev. Lett. **82**, 1233 (1999).

⁷Le Si Dang *et al.*, Phys. Rev. Lett. **81**, 3920 (1998).

⁸P.G. Savvidis *et al.*, Phys. Rev. Lett. **84**, 1547 (2000).

⁹R. Houdré *et al.* (unpublished).

¹⁰T. Usui, Prog. Theor. Phys. **23**, 787 (1960).

¹¹E. Hanamura and H. Haug, Phys. Rep., Phys. Lett. **C33**, 209 (1977).

¹²C. Ciuti *et al.*, Phys. Rev. B **58**, 7926 (1998).

¹³F. Tassone and Y. Yamamoto, Phys. Rev. B **59**, 10 830 (1999).

¹⁴C. Ciuti *et al.*, Phys. Rev. B **58**, R10 123 (1998).

¹⁵G. Rochat *et al.*, Phys. Rev. B **61**, 13 856 (2000).

¹⁶W.H. Louisell, A. Yariv, and A.E. Siegman, Phys. Rev. **124**, 1646 (1961).

¹⁷S. Savasta and R. Girlanda, Phys. Rev. Lett. **77**, 4736 (1996); Phys. Rev. B **59**, 15 409 (1999).